Journal of Fluorine Chemistry 137 (2012) 93–98

Contents lists available at SciVerse ScienceDirect

Journal of Fluorine Chemistry

journal homepage: www.elsevier.com/locate/fluor

Synthesis, characterization and photoluminescence properties of strong fluorescent BF_2 complexes bearing (2-quinolin-2-yl)phenol ligands

Ru-Zheng Ma, Qi-Chao Yao, Xi Yang, Min Xia *

Department of Chemistry, Zhejiang Sci-Tech University, Hangzhou 310018, PR China

ARTICLE INFO

Article history:
Received 16 October 2011
Received in revised form 1 March 2012
Accepted 5 March 2012
Available online 13 March 2012

Keywords:
(2-Quinolin-2-yl)phenols
N,O bidentate BF_2 complexes
Strong fluorescence
Large Stokes shift
High quantum yields
Photophysical properties

ABSTRACT

Novel *N,O* bidentate BF_2 complexes were prepared in good to excellent yields through the coordination of (2-quinolin-2-yl)phenol and its derivatives with boron trifluoride etherate under mild conditions. These fluorine–boron complexes exhibited strong fluorescence both in organic solvents and in solid state. Their photophysical properties were thoroughly studied by absorption and fluorescence spectroscopy in various solvents. The electronic and site effects of substituents on phenolic and quinolinyl rings were found to have a profound impact on quantum yields. All these complexes were fully characterized by IR, ^1H, ^{13}C, ^{19}F NMR and microanalysis. The high quantum yields and large Stokes shifts make these compounds as potential fluorescent dyes.

1. Introduction

The development of highly emissive dyes has been under the focused research recently for their various applications. Among a wide variety of fluorophores, organic difluoroboron complexes are well-known for their strong emission intensity, large extinction coefficients, high quantum yields, outstanding chem- and photostability. Owning to these distinguished characteristics, BF_2 complexes have the broad applications in photodynamic therapy [1,2], as electron-transport materials [3,4], fluorescent biolabels [5,6], chemosensors [7,8] as well as photo sensitizers [9,10]. There are mainly three types of these fluorine–boron complexes, classified as *N,N* bidentate, *O,O* bidentate and *N,O* bidentate compounds. For the former two kinds which have been well documented and thoroughly studied, BODIPY (boradipyrromethene) [11–17] and 1,3-dioxa-2-borine [18–25] are their corresponding representatives. However, *N,O* bidentate complexes, the isosteric analogues to the above two types, have been rarely reported [26–29], especially those with visible fluorescence [30–32].

In our previous work, we found that heterocyclic β-enaminoketones like 3-(2-oxo-2-aryl-ethylidene)-3,4-dihydro-1*H*-quinoxalin-2-ones and 3-(2-oxo-2-arylethylidene)-3,4-dihydrobenzo-[1,4]oxazin-2-ones could be easily exploited as the effective ligands to form the *N,O* bidentate difluoroboron complexes with strong green fluorescence and extraordinarily high quantum yields (>60%) [33]. Inspired by these interesting findings, we were motivated to discover other novel *N,O* bidentate BF_2 complexes with remarkable visible fluorescence characteristics.

(2-Quinolin-2-yl)phenol, which has a phenolic oxygen atom and a quinolinyl nitrogen atom in the same molecular framework and is capable of forming a six-membered chelate ring with an electron-deficient center, is considered as a potential candidate for the coordination with BF_2 on *N,O* anchors. Fortunately, these corresponding BF_2 complexes exhibited characteristics such as strong emission intensity, high quantum yield, large Stokes shift, great absorption coefficient and robust chemical stability. It is worth noting that the variation of substituents on phenolic or quinolinyl rings was found to have a profound impact on the photophysical performance of such BF_2 chelates. Herein we demonstrated the synthesis, structural analysis and spectroscopic behaviors of these BF_2 complexes bearing (2-quinolin-2-yl)phenol ligands. In addition, their photophysical behaviors were thoroughly studied in various solvents as well.

2. Results and discussion

2.1. Synthesis of complexes (6a–i)

In order to obtain the desired ligands (**5a–i**), two routes (Scheme 1) were adopted depending on the different reactivity of the acetyl group on the substituted 2-hydroxyacetophenones (**1**). In cases where R_3 and R_4 were not electron-donating groups, the

* Corresponding author. Tel.: +86 571 86843757; fax: +86 571 86843757.
E-mail address: xiamin@zstu.edu.cn (M. Xia).

0022-1139/$ – see front matter © 2012 Elsevier B.V. All rights reserved.
doi:10.1016/j.jfluchem.2012.03.006

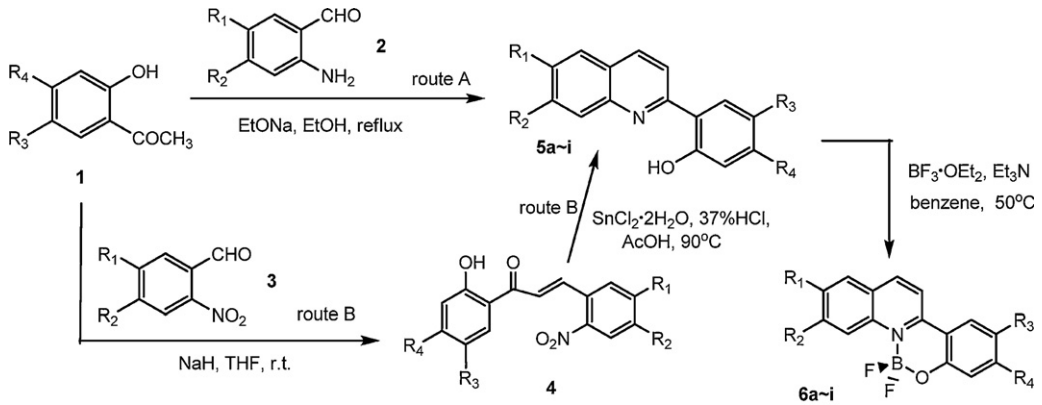

6a: R_1=OCH_3, R_2= OCH_3, R_3=H, R_4=H; **6b**: R_1=H, R_2= Cl, R_3=H, R_4=H

6c: R_1=H, R_2= H, R_3=H, R_4=H; **6d**: R_1=H, R_2= H, R_3=NO_2 R_4=H

6e: R_1=H, R_2= H, R_3=Br, R_4=H; **6f**: R_1=OCH_3, R_2= OCH_3, R_3=NO_2, R_4=H

6g: R_1=H, R_2= H, R_3=CH_3, R_4=H; **6h**: R_1=H, R_2= H R_3=H, R_4=CH_3

6i: R_1=H, R_2= H, R_3=H, R_4=OCH_3

Scheme 1. Route to synthesis of ligands and complexes.

corresponding ligands (**5a**–**f**) could be prepared through the classical Friedländer reaction (route A) [34], in which substituted 2-hydroxyacetophenones and substituted 2-aminobenzaldehydes (**2**) were combined under strong basic conditions. However, when R_3 and R_4 were electron-rich groups, the desired products could not be gained in Friedländer condensation due to the decrease of acetyl reactivity. So another two-step strategy (route B) had to be utilized [35], in which the intermediates 2′-hydroxy-2-nitrochalcones (**4**) were formed in basic medium and underwent the subsequent reductive coupling under acidic condition to form the target ligands (**5g**–**i**).

When 2-(quinolin-2-yl)phenol and its derivatives (**5a**–**i**) were treated with excessive boron trifluoride etherate in the presence of triethylamine, the novel BF_2 complexes (**6a**–**i**) were generated rapidly as yellowish or bright yellow microcrystals in good to excellent yields. These compounds had robust chemical stability, for their solids could be kept for several weeks without isolation from air and moisture. More importantly, their fluorescence in organic solutions was also insensitive to moisture.

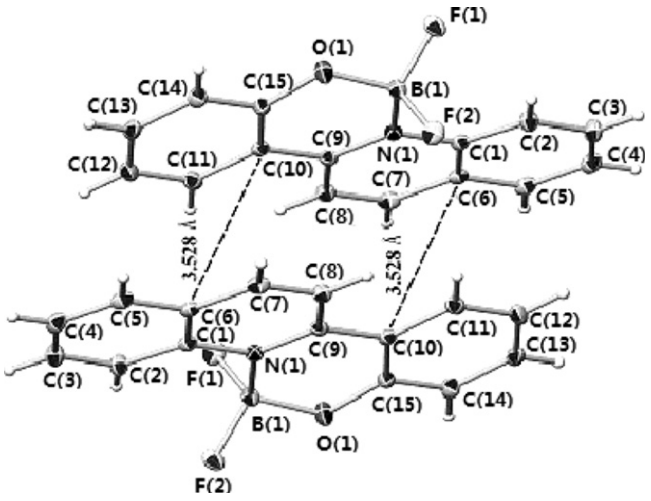

Fig. 1. Molecular structure and π–π stacking interaction of complex **6c**.

2.2. Structural analysis

As all the complexes were of similar structures, complex **6c** was selected as a representative to carry out X-ray single crystal diffraction study and its molecular structure is presented in Fig. 1.

The crystallographic data [36] clearly showed that there was a quite small dihedral angle (about 10°) between C_2–C_9 plane and C_{10}–C_{15} plane due to the chelation of the BF_2 group with 2-(quinolin-2-yl)phenol ligand. Such great improvement of planarity imposed by the chelation led to the more effective linkage between the conjugative regions that were located on phenolic and quinolinyl rings. The extended π-electron delocalization on the complexes was probably responsible for the variations of spectroscopic and photophysical properties from those of the ligands. Additionally, the excellent molecular planarity presented the fully efficient *face-to-face* interaction when the molecules were aggregated in the solid state. Meanwhile, the distance (3.528 Å) between the two molecular planes was extraordinarily short. These elements could result in the strong π–π stacking interaction of the complexes.

Compared with the ligands, the melting points of the complexes were elevated by nearly 100 °C correspondingly. Such a substantial increase could be mainly attributed into two factors by the introduction of the BF_2 group: (i) the largely strengthened dipole–dipole interaction due to the formation of zwitterions; (ii) the much tighter π–π stacking interaction due to the enhanced planarity of the molecules.

2.3. Spectroscopic behavior studies

In comparing the IR spectra of the ligands and the complexes, the most obvious difference was the appearance of strong vibrations in 1000–1200 cm^{-1} region for complexes. This was one of the most powerful pieces of evidence that the BF_2 moiety was successfully grafted into the complexes, as the tetravalent B–F bond possesses its characteristic frequency in this region [37]. Moreover, the B–N vibrations (~920 cm^{-1}) [38] with moderate intensity appeared in the IR spectra of the complexes. The occurrence of these peaks could be also attributed to the effects of the coordination.

Additionally, the disappearance of the downfield hydroxyl proton signals from the ^1H NMR spectra of the complexes was

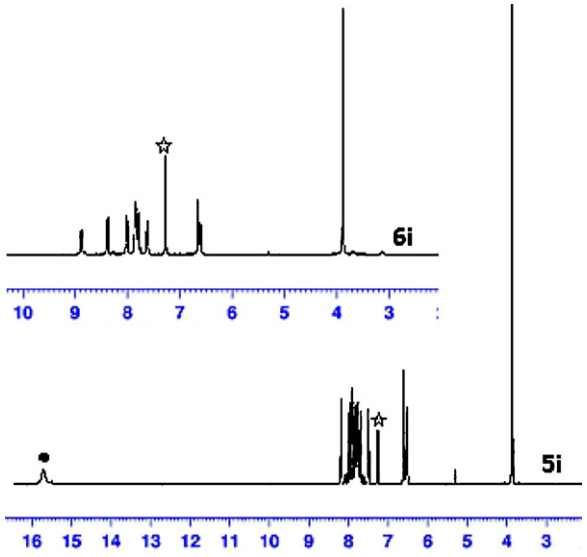

Fig. 2. ^{1}H NMR spectra of ligand **5i** and complex **6i** ($CDCl_3$; proton of hydroxyl on **5i**).

another solid proof for the chelation of the BF_2 group with the ligands. Moreover, due to the generation of permanently positive charges on the N atoms of the complexes, the resulted deshielding effect occurred on the protons and the carbon atoms to some extent through the conjugation. This resulted in the changes of split features for some signals and downfield shifts of whole signals in the ^{1}H NMR spectrum of a given complex, compared with signals of the corresponding ligand. The ^{1}H NMR spectra of ligand **5i** and complex **6i** are shown in Fig. 2. It clearly illustrated that all of the signals moved toward down field to a discernible degree after the coordination. Similarly, the downfield shifts of the ^{13}C signals could also be clearly observed in the ^{13}C NMR spectra of the complexes. However, the detailed assignment of the ^{1}H and ^{13}C signals of complexes was much more difficult.

The ^{19}F NMR spectra displayed a single quartet resonance in nearly 1:1:1:1 area ratio, which revealed that the difluoroboron chelates achieved more symmetric conformations in exchange-averaged solution structures than in the ring-puckered static solid structures due to the fast ring-flipping processes. This spectral feature was similar to the results that were gained in Gardinier's detailed investigation on the ^{19}F NMR spectra of BF_2 complexes [27]. In contrast to our BF_2 complexes, the ^{19}F NMR spectra of *O*,*O* bidentate BF_2 systems with 1,3-diketone ligands [39] showed two sharp lines while and *N*,*N* bidentate BF_2 complexes with benzimidazole ligands [38] exhibited two broad signals. Both of them had the 1:4 integration resonances in accord with the natural abundance of boron isotopes. According to Gardinier's assumption, the vanished B–F couplings in the above two cases could be presumably due in part to the fast relaxation of the quadrupolar boron nucleus [48,49]. Furthermore, it was demonstrated from Table 1 that the ^{19}F chemical shifts were sensitive to the electronic environments of the quinolinyl and phenolic rings. For complexes with electron-rich groups on either the phenolic or the quinolinyl rings, their ^{19}F signals exhibited the upfield shifts. For a given group, as its capability of donating electrons increased, the ^{19}F signal of its corresponding complex had a greater downfield shift. For complex **6g** and **6h**, the different sites of methyl group on the phenolic ring produced the distinct ^{19}F chemical shifts. Moreover, the ^{11}B–^{19}F coupling constants of our BF_2 complexes were in the range of 15.0–18.8 Hz, which were smaller than those (26.3–30.0 Hz) in our early reported cases [33] but agreed well with those in Itoh's β-enaminoketone complexes (17.1–17.9 Hz) [40] and Flores–Parra's benzimidazole complex (16.9 Hz) [38].

2.4. Photophysical property investigations

The UV–Vis absorption and fluorescence data of the ligands and the complexes are listed in Table 1. For absorption spectra, remarkable red shifts of absorption peaks occurring from the ligands to the complexes could be observed. Such red-shift effect might be attributed to the dramatically extended delocalization of conjugative electrons due to the improved planarity in the complexes, which led to the increased energy levels of the HOMOs in ground states and the decreased energy levels of the LUMOs in excited states. Moreover, all of the complexes had the high molar extinction coefficients, which suggested that largely permitted π–π^* electronic transitions occurred during the excitation of the complexes. The absorption spectra of ligand **5i** and complex **6i** are illustrated in Fig. 3.

Although the ligands did not show any fluorescence, the complexes exhibited the intense fluorescence in their organic solutions. The photographs of complex **6a**, **6g** and **6i** in the $CHCl_3$ solutions under daylight and a 365 nm ultraviolet lamp are shown in Fig. 4.

The difference of fluorescence properties between the ligands and the complexes was caused by the increase in rigidity of the 2-(quinolin-2-yl)phenol skeleton of complexes due to the chelation of the boron atoms. This reduced the loss of energy via radiationless thermal vibrations [41]. A correlation could be established between the quantum yields and the substituent groups. Complexes with electron-donating groups had impressively high quantum yields (**6a**, **6c**, **6g–i**) while those with electron-withdrawing groups possessed less (**6b**, **6e**) or even

Table 1
^{19}F NMR chemical shifts and photophysical properties of ligands and complexes.[a]

Entry	λ_{abs} (nm)[b]		Log ε (L/(mol cm))	λ_{em} (nm)		Stokes shift (nm)	Φ (%)[d] (solution)	δ (ppm) in ^{19}F NMR
	Ligand	Complex		Solid	Solution[c]			
a	361	385	4.43	454	441	56	81	−132.96
b	353	381	4.20	484	477	96	31	−131.07
c	348	380	4.13	487	463	83	48	−131.04
d	343	363	4.00	–	–	–	<1	−130.06
e	350	382	3.98	–	482	100	13	−131.01
f	361	396	4.36	–	–	–	<1	−131.99
g	355	387	4.06	489	492	105	57	−131.31
h	351	382	4.23	469	464	82	77	−131.08
i	357	394	4.44	502	458	64	86	−132.14

[a] Both the absorption and emission spectra were measured in $CHCl_3$ solution.
[b] The absorption spectra were determined in $\sim 5.0 \times 10^{-5}$ M solution.
[c] The emission spectra were determined in $\sim 2.0 \times 10^{-7}$ M solution.
[d] The quantum yield was obtained by using quinine sulfate as the standard.

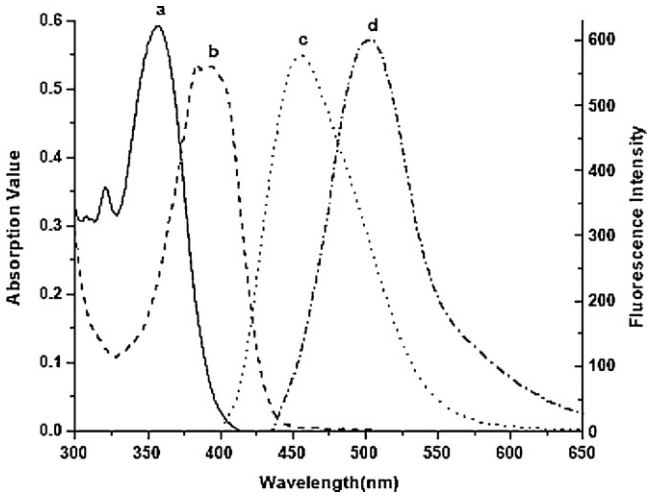

Fig. 3. Spectra of ligand **5i** and **6i** (a: UV–Vis absorption of ligand **5i** in $CHCl_3$ solution; b: UV–Vis absorption of complex **6i** in $CHCl_3$ solution; c: fluorescence emission of complex **6i** in $CHCl_3$ solution; d: fluorescence emission of complex **6i** in solid state).

nearly to zero (**6d**, **6f**) quantum yields. It was assumed that the groups on the phenolic rings were more influential on quantum yields than those on the quinolinyl rings. For example, due to a nitro group on the phenolic ring, both complexes **6f** and **6d** had nearly zero quantum yields in spite of two methoxyl groups on the quinolinyl ring for complex **6f**. Similar case for complexes **6a** and **6f**, the quantum yields were dramatically reduced from 81% for **6a** to <1% for **6f** when a nitro group was introduced on the phenolic ring of complex **6f**. Probably due to the heavy-atom effect which caused an intersystem crossing to a nonradiative triplet state [42], complex **6e** which contained a bromo group at the quinolinyl ring showed a largely decreased quantum yield. Undoubtedly, an improved quantum yield could be gained whether an electron-donating group was located on the quinolinyl or the phenolic ring. It was interesting to notice that the complexes with the different substitution positions of the same group on the phenolic ring gave the different quantum yields, just like the case of complexes **6g** and **6h**.

The emission spectrum of **6i** in solution is presented in Fig. 3. The excellent mirror image relationship between the absorption and the emission spectra of the complexes demonstrated that the distribution of the vibration energy levels in the S_0 states was analogous to that in the S_1 excited states. Compared with the widely observed small Stokes shifts of typical BODIPYs [43], the large shift values in the range of 56–105 nm for our complexes were quite impressive and promised to be helpful for the further applications.

Table 2
Photophysical properties of complex **6c** in different solvents.

Entry	Solvent	λ_{abs} (nm)[a]	λ_{em} (nm)[b]	$\Delta\lambda$ (nm)
1	Benzene	381	461	80
2	THF	377	464	87
3	CH_2Cl_2	376	465	89
4	Dioxane	376	470	94
5	Acetone	365	481	116
6	Acetonitrile	364	487	123
7	Methanol	345	–	–

[a] The absorption spectra were determined in $\sim 5.0 \times 10^{-5}$ M solution.
[b] The emission spectra were determined in $\sim 2.0 \times 10^{-7}$ M solution.

Unlike the typical BODIPYs which hardly fluoresce in solid state [44], the complexes with fairly strong emission in solutions could exhibit fluorescence in the solid state as well. It was assumed that large Stokes shifts partly offset the self-quenching effect in the solid state [45]. The emission maxima underwent the remarkable red shifts in the solid state, which could be attributed to the π–π stacking induced by the more compact molecular aggregation in the solid state.

The photophysical characteristics of complex **6c** in various solvents are tested and the results are listed in Table 2. The absorption maximum underwent a hypsochromic shift with an increase in solvent polarity. Such solvent-dependent behavior was similar to the reported 1,3-enaminoketonatoboron difluorides [40] and implied that the peaks originated from the π–π^* transition. Among all the investigated solvents, the blue shift up to 36 nm could be observed between the absorption bands measured in benzene and methanol.

The solvent-dependent correlation was also revealed from the emission spectra and the solvent polarity, since it was found that the peak gradually went through a bathochromic shift as the polarity of the solvent increased. Among all the employed solvents, the longest wavelength was at 487 nm in acetonitrile and the shortest one was at 461 nm in benzene. For BF_2 complexes, the excited states are usually species with the larger dipole moments than the corresponding ground states due to the rearrangement of the excited electrons [46]. Therefore, the contribution of solvation to the stabilization of excited state is much larger than that of ground state, and such solvation effect is much greater in solvents with higher polarity than in ones with lower polarity. Thus, a red-shift emission is resulted when the electrons from the stabilized excited state fall back to the ground state. However, the solution fluorescence was completely quenched in methanol; this might be due to a strong interaction to form an H-bond complex between the protic solvent and the excited state [47]. The Stokes shifts turned over 80 nm and the largest one was observed for 123 nm in acetonitrile. The large Stokes shifts remarkably alleviated the self-absorption and were beneficial for the performance of intense fluorescence.

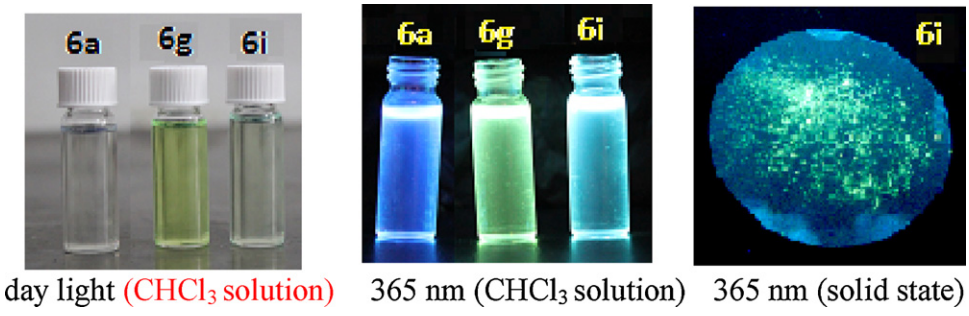

Fig. 4. The photographs of samples in solution and in solid state.

3. Conclusion

Herein we described the synthesis, structural analysis, spectral and photophysical property studies of the novel BF_2 complexes bearing 2-(quinolin-2-yl)phenol ligands. The preparation of these complexes was performed in good to excellent yields under mild conditions with simple work-up procedures. These dyes displayed solvent-sensitive absorption and emission features. The electronic and site effect of substituents played an important role in the quantum yields of the corresponding complexes. The strong emission in solutions and in solid state as well as the impressive large Stokes shifts and the high quantum yields made these compounds as useful fluorescent materials. Further work on the development of their potential applications is underway and will be reported soon.

4. Experimental

4.1. Apparatus and materials

All the reagents used were analytically pure and some chemicals were further purified by recrystallization or distillation. Melting points were determined by a X-4 micro melting instrument and the thermometer was uncorrected. The ^{1}H NMR (400 MHz), ^{13}C NMR (100 MHz) and ^{19}F NMR (376 MHz) spectra were obtained on a Bruker Avance II DMX400 spectrometer using $CDCl_3$ or DMSO-d_6 as the solvent. The ^{1}H NMR and ^{13}C NMR experiments were carried out using trimethylsilane as the internal standard and the ^{19}F NMR spectra were recorded using CF_3COOH (−76.5 ppm) as the external standard. FT-IR spectra were performed using KBr pellets on a Nicolet Avatar spectrophotometer. The absorption spectra were measured on a Shimadzu UV 2501(PC)S UV–Vis spectrometer and the fluorescence spectra were acquired on a Perkin-Elmer LS55 spectrophotometer.

4.2. General procedure for synthesis of complex (6a–i)

At room temperature, triethylamine (2 mmol) was added to the solution of ligand (1 mmol) in benzene (3 mL), the resulted mixture was stirred for 20 min and then boron trifluoride etherate (3 mmol) was added. The mixture was stirred at 50 °C for 1 h and yellowish solid was gradually precipitated out from the solution. After cooling to room temperature, the mixture was filtrated and the solid was washed several times by ether and dried in air. For microanalysis, the solid was recrystallized in the benzene/hexane mixture.

Complex **6a**: 81% yield, m.p. 272–273 °C; IR (KBr): ν 1622 (C=N), 1556 (C=C), 1110 (B–F), 923 (B–N) cm^{-1}; ^{1}H NMR (400 MHz, $CDCl_3$): δ 4.02 (s, 3H), 4.14 (s, 3H), 7.00 (m, 1H), 7.03 (m, 1H), 7.18 (m, 1H), 7.46 (t, 1H, J = 7.6 Hz), 7.82 (d, 1H, J = 8.0 Hz), 7.93 (d, 1H, J = 8.8 Hz), 8.28 (m, 2H); ^{13}C NMR (100 MHz, DMSO-d_6): δ 56.20, 56.62, 104.45, 105.70, 114.90, 116.38, 120.04, 120.29, 124.06, 126.12, 134.48, 137.67, 140.46, 149.81, 150.44, 154.55, 155.41; Found: C, 61.88; H, 4.21; N, 4.19; Anal. Calc. for $C_{17}H_{14}NOBF_2$: C, 61.98; H, 4.25; N, 4.25%.

Complex **6b**: 76% yield, m.p. 262–264 °C; IR (KBr): ν 1614 (C=N), 1586 (C=C), 1099 (B–F), 930 (B–N) cm^{-1}; ^{1}H NMR (400 MHz, $CDCl_3$): δ 7.04 (m, 1H), 7.19 (m, 1H), 7.54 (t, 1H, J = 7.6 Hz), 7.62 (d, 1H, J = 8.4 Hz), 7.83 (m, 2H), 8.13 (d, 1H, J = 8.8 Hz), 8.46 (d, 1H, J = 8.8 Hz), 8.96 (m, 1H); ^{13}C NMR (100 MHz, DMSO-d_6): δ 117.31, 120.43, 120.67, 124.18, 124.28, 124.38, 125.97, 126.87, 129.24, 129.47, 136.12, 139.66, 142.43, 153.57, 156.44; Found: C, 59.39; H, 3.01; N, 4.56; Anal. Calc. for $C_{15}H_9NOBF_2Cl$: C, 59.31; H, 2.96; N, 4.61%.

Complex **6c**: 86% yield, m.p. 264–265 °C; IR (KBr): ν 1609 (C=N), 1560 (C=C), 1085 (B–F), 922 (B–N) cm^{-1}; ^{1}H NMR (400 MHz, $CDCl_3$): δ 7.04 (m, 1H), 7.08 (m, 1H), 7.54 (t, 1H, J = 8.0 Hz), 7.69 (d, 1H, J = 7.6 Hz), 7.89 (m, 3H), 8.17 (t, 1H, J = 8.8 Hz), 8.51 (d, 1H, J = 8.8 Hz), 8.95 (d, 1H, J = 9.2 Hz); ^{13}C NMR (100 MHz, DMSO-d_6): δ 117.08, 120.34, 120.47, 124.84, 124.92, 126.74, 127.64, 128.06, 128.41, 132.98, 135.64, 140.36, 142.81, 152.83, 156.39; Found: C, 66.83; H, 3.75; N, 5.16; Anal. Calc. for $C_{15}H_{10}NOBF_2$: C, 66.90, H, 3.72; N, 5.20%.

Complex **6d**: 71% yield, m.p. > 300 °C; IR (KBr): ν 1615 (C=N), 1553 (C=C), 1117 (B–F), 929 (B–N) cm^{-1}; ^{1}H NMR (400 MHz, $CDCl_3$): δ 7.35 (d, 1H, J = 8.8 Hz), 7.91 (t, 1H, J = 7.6 Hz), 8.11 (t, 1H, J = 7.6 Hz), 8.39 (d, 1H, J = 8.4 Hz), 8.47 (d, 1H, J = 9.2 Hz), 8.71 (d, 1H, J = 8.4 Hz), 8.96 (d, 1H, J = 8.4 Hz), 9.14 (d, 1H, J = 9.2 Hz), 9.26 (s, 1H); ^{13}C NMR (100 MHz, DMSO-d_6): δ 118.48, 118.78, 118.95, 124.31, 126.88, 126.94, 127.27, 128.06, 131.29, 139.07, 139.42, 143.56, 155.56, 155.43, 165.96; Found: C, 57.25; H, 2.90; N, 8.86; Anal. Calc. for $C_{15}H_9N_2O_3BF_2$: C, 57.31; H, 2.86; N, 8.91%.

Complex **6e**: 77% yield, m.p. 294–295 °C; IR (KBr): ν 1607 (C=N), 1555 (C=C), 1089 (B–F), 927 (B–N) cm^{-1}; ^{1}H NMR (DMSO-d_6): δ 6.99 (d, 1H, J = 8.8 Hz), 7.54 (d, 1H, J = 8.8 Hz), 7.70 (t, 1H, J = 7.2 Hz), 7.87 (t, 1H, J = 8.4 Hz), 8.10 (t, 2H, J = 8.4 Hz), 8.37 (s, 1H), 8.45 (d, 1H, J = 8.8 Hz), 8.63 (d, 1H, J = 8.8 Hz); ^{13}C NMR (100 MHz, DMSO-d_6): δ 110.11, 118.58, 120.17, 120.92, 126.65, 126.90, 127.36, 127.99, 130.18, 131.12, 134.52, 138.77, 143.81, 156.07, 159.02; Found: C, 51.67; H, 2.52; N, 4.06; Anal. Calc. for $C_{15}H_9NOBF_2Br$: C, 51.73; H, 2.58; N, 4.02%.

Complex **6f**: 84% yield, m.p. > 300 °C; IR (KBr): ν 1621 (C=N), 1543 (C=C), 1095 (B–F), 929 (B–N) cm^{-1}; ^{1}H NMR (400 MHz, $CDCl_3$): δ 4.00 (s, 6H), 7.31 (d, 1H, J = 9.2 Hz), 7.75 (m, 1H), 8.04 (m, 1H), 8.39 (d, 1H, J = 7.6 Hz), 8.71 (m, 1H), 8.88 (d, 1H, J = 8.8 Hz), 9.14 (m, 1H); ^{13}C NMR (100 MHz, DMSO-d_6): δ 56.08, 56.13, 102.67, 107.09, 116.33, 116.48, 120.06, 123.95, 125.20, 129.17, 136.48, 140.84, 142.58, 146.74, 150.49, 154.63, 159.25; Found: C, 54.47; H, 3.51; N, 7.42; Anal. Calc. for $C_{17}H_{13}N_2O_5BF_2$: C, 54.53; H, 3.47; N, 7.48%.

Complex **6g**: 91% yield, m.p. 264–265 °C; IR (KBr): ν 1620 (C=N), 1560 (C=C), 1100 (B–F), 920 (B–N) cm^{-1}; ^{1}H NMR (DMSO-d_6): δ 2.39 (s, 3H), 7.11 (d, 1H, J = 8.4 Hz), 7.35 (d, 1H, J = 8.8 Hz), 7.67 (m, 2H), 7.89 (m, 2H), 8.16 (d, 1H, J = 8.8 Hz), 8.49 (d, 1H, J = 8.8 Hz), 8.95 (d, 1H, J = 9.6 Hz); ^{13}C NMR (100 MHz, DMSO-d_6): δ 20.84, 117.11, 120.07, 124.71, 124.80, 124.89, 126.45, 127.56, 127.93, 128.37, 129.63, 132.89, 136.84, 142.64, 152.88, 154.33; Found: C, 67.91; H, 4.19; N, 5.01; Anal. Calc. for $C_{16}H_{12}NOBF_2$: C, 67.82; H, 4.24; N, 4.95%.

Complex **6h**: 94% yield, m.p. 257–259 °C; IR (KBr): ν 1616 (C=N), 1553 (C=C), 1086 (B–F), 909 (B–N) cm^{-1}; ^{1}H NMR (DMSO-d_6): δ 2.40 (s, 3H), 6.84 (d, 1H, J = 8.0 Hz), 7.00 (s, 1H), 7.64 (t, 1H, J = 7.6 Hz), 7.76 (d, 1H, J = 8.4 Hz), 7.87 (t, 2H, J = 7.6 Hz), 8.08 (d, 1H, J = 8.8 Hz), 8.43 (d, 1H, J = 8.8 Hz), 9.92 (d, 1H, J = 8.8 Hz); ^{13}C NMR (100 MHz, DMSO-d_6): δ 21.25, 118.04, 118.17, 119.03, 121.91, 123.15, 127.44, 127.90, 128.03, 129.27, 132.05, 139.01, 143.96, 146.95, 152.32, 155.31; Found: C, 67.86; H, 4.28; N, 4.89; Anal. Calc. for $C_{16}H_{12}NOBF_2$: C, 67.82; H, 4.24; N, 4.95%.

Complex **6i**: 83% yield, m.p. 243–244 °C; IR (KBr): ν 1617 (C=N), 1557 (C=C), 1109 (B–F), 910 (B–N) cm^{-1}; ^{1}H NMR (DMSO-d_6): δ 3.88 (s, 3H), 6.62 (m, 2H), 7.61 (t, 1H, J = 7.6 Hz), 7.84 (m, 3H), 8.00 (d, 1H, J = 9.2 Hz), 8.37 (d, 1H, J = 9.2 Hz), 8.87 (d, 1H, J = 8.8 Hz); ^{13}C NMR (100 MHz, DMSO-d_6): δ 55.69, 102.51, 110.03, 116.69, 124.29, 124.38, 124.47, 126.98, 127.43, 128.08, 128.35, 132.73, 142.19, 152.65, 158.73, 166.06; Found: 64.28; H, 3.96; N, 4.72; Anal. Calc. for $C_{16}H_{12}NO_2BF_2$: C, 64.20; H, 4.01; N, 4.68%.

Acknowledgments

We are grateful for the financial support from the Natural Science Foundation of Zhejiang Province (Y4100034) and Zhejiang Provincial Key Innovation Team (2010R50038).

References

[1] S. Ozlem, E.U. Akkaya, J. Am. Chem. Soc. 131 (2009) 48–49.
[2] S. Erbas, A. Gorgulu, M. Kocakusakogullari, E.U. Akkaya, Chem. Commun. (2009) 4956–4958.
[3] C.D. Entwistle, T.B. Marder, Chem. Mater. 16 (2004) 4574–4585.
[4] Y. Li, Y. Liu, W. Bu, J. Guo, Y. Wang, Chem. Commun. (2000) 1551–1552.
[5] M. Sameiro, T. Goncalves, Chem. Rev. 109 (2009) 190–212.
[6] D. Wang, J. Fan, X. Gao, B. Wang, S. Sun, X. Peng, J. Org. Chem. 74 (2009) 7675–7683.
[7] I. Mócázr, P. Huszthy, Z. Maidics, M. Kádár, K. Tóth, Tetrahedron 65 (2009) 8250–8258.
[8] R. Guliyev, O. Buyukcakir, F. Sozmen, O.A. Bozdemir, Tetrahedron Lett. 50 (2009) 5139–5141.
[9] S. Erten-Ela, M.D. Yilmaz, B. Icli, Y. Dede, S. Icli, E.U. Akkaya, Org. Lett. 10 (2008) 3299–3302.
[10] S. Hattori, K. Ohkubo, Y. Urano, H. Sunahara, T. Nagano, Y. Wada, N.V. Tkachenko, H. Lemmetyinen, S. Fukuzumi, J. Phys. Chem. B 109 (2005) 15368–15375.
[11] A. Loudet, K. Burgess, Chem. Rev. 107 (2007) 4891–4932.
[12] G. Ulrich, R. Ziessel, A. Harriman, Angew. Chem. Int. Ed. 47 (2008) 1184–1201.
[13] R. Ziessel, G. Ulrich, A. Harriman, New J. Chem. 31 (2007) 496–501.
[14] D.W. Domaille, L. Zeng, C.J. Chang, J. Am. Chem. Soc. 132 (2010) 1194–1195.
[15] S. Atilgan, I. Kutuk, T. Ozdemir, Tetrahedron Lett. 51 (2010) 892–894.
[16] R. Ziessel, G. Ulrich, A. Harriman, M.A.H. Alamiry, B. Stewart, P. Retailleau, Chem. Eur. J. 15 (2009) 1359–1369.
[17] M. Baruah, W. Qin, N. Basaric, W.M. De Borggraeve, N. Boens, J. Org. Chem. 70 (2005) 4152–4157.
[18] Y.L. Chow, C.I. Johansson, Y.-H. Zhang, R. Gautron, L. Yang, A. Rassat, S.-Z. Yang, J. Phys. Org. Chem. 9 (1996) 7–16.
[19] G.Q. Zhang, J.B. Chen, S.J. Payne, S.E. Kooi, J.N. Demas, C.L. Fraser, J. Am. Chem. Soc. 129 (2007) 8942–8943.
[20] K. Ono, K. Yoshikawa, Y. Tsuji, H. Yamaguchi, R. Uozumi, M. Tomura, K. Taga, K. Saito, Tetrahedron 63 (2007) 9354–9358.
[21] K. Zyabrev, A. Doroshenko, E. Mikitenko, Y. Slominskii, A. Tolmachev, Eur. J. Org. Chem. (2008) 1550–1558.
[22] E.V. Fedorenko, B.V. Bukvetskii, A.G. Mirochnik, D.H. Shlyk, M.V. Tkacheva, A.A. Karpenko, J. Lumin. 130 (2010) 756–761.
[23] A.O. Gerasov, M.P. Shandura, Y.P. Kovtun, Dyes Pigm. 79 (2008) 252–258.
[24] D. Rohde, C.-J. Yan, L.-J. Wan, Langmuir 22 (2006) 4750–4757.
[25] M. Guerro, T. Roisnel, D. Lorcy, Tetrahedron 65 (2009) 6123–6127.
[26] K. Itoh, K. Okazaki, Y.L. Chow, Helvet. Chim. Acta 87 (2004) 292–302.
[27] F.P. Macedo, C. Gwengo, S.V. Lindeman, M.D. Smith, J.R. Gardinier, Eur. J. Inorg. Chem. (2008) 3200–3211.
[28] M. Guerro, T.D. Dama, S. Bakhta, B. Kolli, T. Roisnel, D. Lorcy, Tetrahedron 67 (2011) 3427–3433.
[29] K. Itoh, M. Fujimoto, M. Hashimoto, New J. Chem. 26 (2002) 1070–1075.
[30] N. Tolle, U. Dunkel, L. Oehninger, I. Ott, L. Preu, T. Haase, S. Behrends, P.G. Jones, F. Totzke, C. Schächtele, M.H.G. Kubbutat, C. Kunick, Synthesis (2011) 2848–2858.
[31] Y. Zhou, Y. Xiao, S.M. Chi, X.H. Qian, Org. Lett. 10 (2008) 633–636.
[32] J.Q. Feng, B.L. Liang, D.L. Wang, L. Xue, X.Y. Li, Org. Lett. 10 (2008) 4437–4440.
[33] M. Xia, B. Wu, G.F. Xiang, J. Fluorine Chem. 129 (2008) 402–408.
[34] C.C. Chen, S.J. Yang, Org. React. 28 (1982) 37–43.
[35] A.I.R.N.A. Barros1, A.F.R. Diasl, A.M.S. Silva, Monatsh. Chem. 138 (2007) 585–594.
[36] X. Yang, M. Xia, Acta Crystallogr. E E67 (2011) 1049.
[37] G.W. Gokel, Dean's Handbook of Organic Chemistry, 2nd ed., McGraw-Hill Companies, 2004.
[38] A. Esparza-Ruiz, A. Peña-Hueso, H. Nöth, A. Flores-Parra, R. Contreras, J. Organomet. Chem. 694 (2009) 3814–3822.
[39] N.M.D. Brown, P. Bladon, J. Chem. Soc. A (1969) 526–532.
[40] K. Itoh, K. Okazaki, M. Fujimoto, Aust. J. Chem. 56 (2003) 1209–1214.
[41] C. Ikeda, S. Ueda, T. Nabeshima, Chem. Commun. (2009) 2544–2546.
[42] A. Gorman, J. Killoran, C. O'Shea, T. Kenna, W.M. Gallagher, D.F. O'Shea, J. Am. Chem. Soc. 126 (2004) 10619–10631.
[43] H. Martin, H. Rudolf, F. Vlastimil (Eds.), Fluorescence Spectroscopy in Biology: Advanced Methods and their Applications to Membranes, Proteins, DNA, and Cells, Springer-Verlag, Heidelberg, Germany, 2005.
[44] D. Zhang, Y. Wen, Y. Xiao, G. Yu, Y. Liu, X. Qian, Chem. Commun. (2008) 4777–4779.
[45] Y. Zhou, Y. Xiao, D. Li, M. Fu, X. Qian, J. Org. Chem. 73 (2008) 1571–1574.
[46] W.W. Qin, M. Baruah, M. Van der Auweraer, F.C. De Schryver, N. Boens, J. Phys. Chem. A 109 (2005) 7371–7384.
[47] Z.R. Grabowski, K. Rotkiewicz, Chem. Rev. 103 (2003) 3899–4032.
[48] N.N. Shapet'ko, L.N. Kurkovskaya, V.G. Medvedeva, A.P. Skoldinov, L.K. Vasyanina, Zh. Strukt. Khim. 10 (1969) 936–942.
[49] J. Bacon, R.J. Gillespie, J.W. Quail, Can. J. Chem. 41 (1963) 3063–3069.